Spin current pumping in helical Luttinger liquids

D. Ferraro[1,2,3], G. Dolcetto[1,2,3], R. Citro[4,5], F. Romeo[4,5], M. Sassetti[1,2]
[1] *Dipartimento di Fisica, Università di Genova,Via Dodecaneso 33, 16146, Genova, Italy.*
[2] *CNR-SPIN, Via Dodecaneso 33, 16146, Genova, Italy.*
[3] *INFN, Via Dodecaneso 33, 16146, Genova, Italy.*
[4] *Dipartimento di Fisica "E. R. Caianiello", Università degli Studi di Salerno, Via Ponte don Melillo, I-84084, Fisciano (Sa), Italy.*
[5] *CNR-SPIN, UO Salerno, Via Ponte don Melillo, I-84084, Fisciano (Sa), Italy.*
(Dated: September 18, 2012)

We study the DC spin current induced into an unbiased quantum spin Hall system through a two-point contacts setup with time dependent electron tunneling amplitudes. By means of two external gates, it is possible to drive a current with spin-preserving and spin-flipping contributions showing peculiar oscillations as a function of pumping frequency, electron-electron interaction and temperature. From its interference patterns as a function of the Fabry-Pérot and Aharonov-Bohm phases, it is possible to extract information about the helical nature of the edge states and the intensity of the electron-electron interaction.

PACS numbers: 73.23.-b, 72.25.Pn, 71.10.Pm

I. INTRODUCTION

In recent years the edge states of two dimensional topological insulators, showing the quantum spin Hall (QSH) effect, have been subject of attention from the condensed matter community.[1] These states have been theoretically predicted in graphene layers with spin-orbit interaction[2,3] and strained semiconductors[4] and experimentally observed in Mercury-Telluride quantum wells[5–7]. Their more relevant feature is the helicity[8], namely the fact that opposite spins propagate in opposite directions along the same edge. As far as time reversal symmetry is preserved, the backscattering between these different spin channels is indeed suppressed.[9]

Various proposals have been done in order to extract information about the helical nature of these states by means of transport measurements. In the simple quantum point contact (QPC) geometry[10] signatures of helicity and electron-electron interaction can be found in the power-low behavior of the spin current as a function of the source-drain voltage in a two terminal configuration.[11] The presence of a single peak of the differential conductance in an extended contact geometry is also a clear signature of the lack of the spin-charge separation typical of these systems.[12] Moreover, by properly tune the voltages in a four terminal configuration it is possible to generate pure charged and spin currents making these systems suitable candidates for the development of spintronic.[13–15]

Extremely interesting are also the interferometric properties of these states. Indeed, in a two QPCs geometry, the presence of external gates can lead to Fabry-Pérot and Aharonov-Bohm oscillations without need of magnetic fields.[16] This fact, together with the possibility of switching the current through the gap in the spectrum induced by the hybridization of the states on opposite edges[17], leads to great advantages in terms of experimental feasibility. In this geometry, with all the terminals unbiased, it is also possible to induce DC spin and charge currents by periodically modulating in time electron tunneling amplitudes or external gate voltages. Such kind of pumping currents have been analyzed in details for the non-interacting case in terms of the scattering matrix formalism in Ref. 18. However the investigation of the interacting case is still an open problem and requires a completely different approach based on the helical Luttinger liquid model.[11,13]

Aim of this paper is to carry out this analysis on the spin current. We will consider a two QPCs geometry in an unbiased four terminal configuration, focusing on the amplitude-modulating tunneling case[18], where a DC spin current can be induced by means of electron tunneling amplitudes periodically modulated in time. We will take into account both spin-preserving (SP) and spin-flipping (SF) contributions admitted by the time-reversal symmetry. Due to the helical properties of the edge states a spin current can be induced only by electrical means, differently from what happens for the spinfull Luttinger liquids, where a magnetic field is required.[19,20] Fabry-Pérot and Aharonov-Bohm interference paths are induced by applying different gate voltages at the opposite edges of the sample. We will focus on the first perturbative order in tunneling. For high enough pumping frequency the effect of the distance between the two QPCs can be taken into account in terms of modulating functions showing oscillations that strongly affect the behavior of the current. The study of such oscillations as a function of the frequency, together with the investigation of the interference patterns as a function of the Fabry-Pérot and Aharonov-Bohm phases, will provide important information about the interaction between the electrons along the edges.

The paper can be divided as follows. In Sec. II we introduce the helical Luttinger liquid description for the edge states of the two dimensional topological insulators. We describe the two QPCs geometry in which a DC spin

current can be generated by means of periodically driven tunneling amplitudes out of phase. For this geometry we analyze the SP and SF contributions to the spin current both at zero and finite temperature by taking into account the presence of the contacts through modulating functions. We discuss the universality of the pumped spin charge as a function of the interaction. In Sec. III we show the behavior of the modulating functions as a function of the pumping frequency for different interaction strengths and temperatures. We than investigate the spin current both by varying the frequency and also as a function of the Fabry-Pérot and Aharonov-Bohm phases induced by the presence of external gates. Sec. IV is devoted to conclusions.

II. MODEL

We investigate a QSH system with a single Kramers doublet of helical edge states. Due to their helical properties[8] one can consider right-moving spin up and left-moving spin down electrons on the top edge (T) and the opposite on the bottom edge (B) (see Fig 1).

The corresponding Hamiltonians for free electrons are[11,13]

$$\begin{aligned}\mathcal{H}_{T(B)} &= -i\hbar v_F \int dx \Big(:\Psi^\dagger_{R,\uparrow(\downarrow)}\partial_x \Psi_{R,\uparrow(\downarrow)} \\ &\quad -\Psi^\dagger_{L,\downarrow(\uparrow)}\partial_x \Psi_{L,\downarrow(\uparrow)}: \Big) \end{aligned} \tag{1}$$

where $\Psi_{R,\uparrow}$ ($\Psi_{L,\uparrow}$) annihilates right (left)-moving electron with spin up, and analogous for the spin down, and v_F is the Fermi velocity. With : ... : we indicate the normal ordering with respect to the equilibrium state where all states below Fermi level are occupied.

Concerning electron-electron interactions, the only admitted terms are the ones that preserve the time-reversal symmetry of the system[21], namely the dispersive

$$\begin{aligned}\mathcal{H}_d &= g_{2\perp}\int dx : \Big(:\Psi^\dagger_{R,\uparrow}\Psi_{R,\uparrow}:: \Psi^\dagger_{L,\downarrow}\Psi_{L,\downarrow}:: \\ &\quad + :\Psi^\dagger_{L,\uparrow}\Psi_{L,\uparrow}:: \Psi^\dagger_{R,\downarrow}\Psi_{R,\downarrow}: \Big) : \end{aligned} \tag{2}$$

and the forward scattering

$$\mathcal{H}_f = \frac{g_{4\parallel}}{2}\sum_{\nu=R,L;\sigma=\uparrow,\downarrow}\int dx : \left(:\Psi^\dagger_{\nu,\sigma}\Psi_{\nu,\sigma}:: \Psi^\dagger_{\nu,\sigma}\Psi_{\nu,\sigma}: \right) : . \tag{3}$$

We will neglect possible Umklapp terms, which are important only at certain commensurate fillings.[8]

Through the standard bosonization technique[22,23] one can write the electronic operators as

$$\Psi_{R,\uparrow}(x) = \frac{\mathcal{F}_{R,\uparrow}}{\sqrt{2\pi\alpha}} e^{ik_F^{(T)}x} e^{-i\sqrt{2\pi}\varphi_{R,\uparrow}(x)} \tag{4}$$

$$\Psi_{L,\downarrow}(x) = \frac{\mathcal{F}_{L,\downarrow}}{\sqrt{2\pi\alpha}} e^{-ik_F^{(T)}x} e^{-i\sqrt{2\pi}\varphi_{L,\downarrow}(x)} \tag{5}$$

$$\Psi_{R,\downarrow}(x) = \frac{\mathcal{F}_{R,\downarrow}}{\sqrt{2\pi\alpha}} e^{ik_F^{(B)}x} e^{-i\sqrt{2\pi}\varphi_{R,\downarrow}(x)} \tag{6}$$

$$\Psi_{L,\uparrow}(x) = \frac{\mathcal{F}_{L,\uparrow}}{\sqrt{2\pi\alpha}} e^{-ik_F^{(B)}x} e^{-i\sqrt{2\pi}\varphi_{L,\uparrow}(x)} \tag{7}$$

with $\varphi_{R/L,\sigma}(x)$ ($\sigma =\uparrow,\downarrow$) bosonic fields, $\mathcal{F}_{R/L,\sigma}$ Klein factors necessary to give the proper commutation relations between electrons belonging to different edges, α finite length cut-off, $k_F^{(T)}$ and $k_F^{(B)}$ Fermi momenta in the top and bottom edge respectively. As a consequence of different gate voltages applied to the edges one has $k_F^{(T)} \neq k_F^{(B)}$ (see Fig. 1).

The bosonic fields $\varphi_{R/L,\sigma}(x)$ are related to the electron density along the edges through[22,23]

$$\rho_{R/L,\sigma}(x) = \mp\frac{1}{\sqrt{2\pi}}\partial_x\varphi_{R/L,\sigma}(x). \tag{8}$$

It is useful to introduce the helical basis for the bosonic fields on the upper and lower edge[23]

$$\varphi_{T(B)}(x) = \frac{1}{\sqrt{2}}\left[\varphi_{L,\downarrow(\uparrow)}(x) - \varphi_{R,\uparrow(\downarrow)}(x)\right], \tag{9}$$

with the canonically conjugated fields

$$\theta_{T(B)}(x) = \frac{1}{\sqrt{2}}\left[\varphi_{L,\downarrow(\uparrow)}(x) + \varphi_{R,\uparrow(\downarrow)}(x)\right]. \tag{10}$$

The total low energy Hamiltonian assumes the typical form of an helical Luttinger liquid[11–13]

$$\mathcal{H}_{eff} = \frac{v}{2}\sum_{i=T,B}\int dx \left[\frac{1}{K}\left(\partial_x\varphi_i\right)^2 + K\left(\partial_x\theta_i\right)^2\right], \tag{11}$$

with $K = \sqrt{\frac{2\pi v_F\hbar + g_{4\parallel} - g_{2\perp}}{2\pi v_F\hbar + g_{4\parallel} + g_{2\perp}}}$ the interaction strength and $v = v_F\sqrt{\left(1+\frac{g_{4\parallel}}{2\pi v_F\hbar}\right)^2 - \left(\frac{g_{2\perp}}{2\pi v_F\hbar}\right)^2}$ the renormalized velocity. In the following we will consider the pure Coulomb repulsion ($g_{4\parallel} = g_{2\perp} > 0$) with $v = v_F/K$ and $K < 1$.

A. Tunneling processes and gates coupling

As shown in Ref. 19, it is possible, in a two QPCs geometry, to induce a DC current in a grounded one-dimensional electron system by means of a quantum pump. Tunneling processes are periodically driven in time, with a proper relative phase. Here, we consider a similar set up for an helical Luttinger liquid in a four terminal configuration, where all the external reservoirs are unbiased.

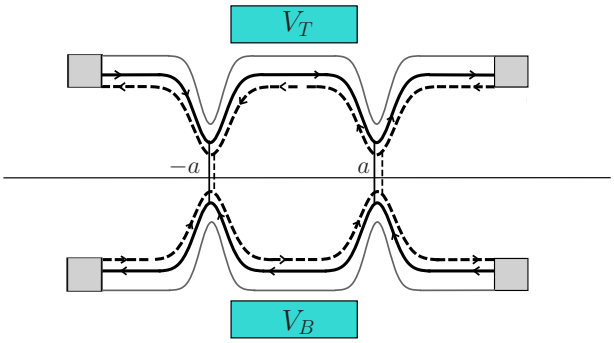

Figure 1: (Color online) Top view of the four terminal interferometric setup. On the top edge one has right-moving spin up electrons (full line) and left-moving spin down electron (dashed line). The opposite holds for the bottom edge. The amplitudes of both SP and SF electron tunneling at the QPCs placed at $x = \pm a$ are modulated in time with frequency ω and phase difference θ. The presence of the top (V_T) and bottom (V_B) gates can lead to a mismatch between the Fermi levels of the two edges ($k_F^{(T)} \neq k_F^{(B)}$). Shaded grey areas indicate the unbiased terminals.

The more general time dependent electron tunneling Hamiltonians that preserve time-reversal symmetry are[18,24]:

$$\mathcal{H}^{sp}(t) = \sum_{\sigma=\uparrow,\downarrow} \hbar \int_{-\infty}^{+\infty} dx \left\{ \gamma_{sp}(x,t) \Psi^{\dagger}_{R,\sigma}(x) \Psi_{L,\sigma}(x) \right\} + \text{h.c.}, \tag{12}$$

and

$$\mathcal{H}^{sf}(t) = \sum_{\nu=R,L} \hbar\xi_{\nu} \int_{-\infty}^{+\infty} dx \left\{ \gamma_{sf}(x,t) \Psi^{\dagger}_{\nu,\uparrow}(x) \Psi_{\nu,\downarrow}(x) \right\} + \text{h.c.}, \tag{13}$$

being $\xi_{R,L} = \pm$, which represent the SP and SF contribution to tunneling respectively. The latter term is strictly zero for inversion symmetric systems due to spin conservation, however gates and deformations of the edges can locally modify the intensity of the spin-orbit interaction leading to spin flipping processes.[25]

In order to generate a DC spin current out of the pump one needs time-dependent tunneling amplitudes. They can be realized by additional periodically driven local electrostatic gates placed at $x = \pm a$

$$\gamma_j(x,t) = \lambda_j \left[\delta(x+a)\cos(\omega t + \theta) + \delta(x-a)\cos(\omega t) \right] \tag{14}$$

with λ_j ($j = sp, sf$) a real parameter according to the requirement of time-reversal invariance, ω the pumping frequency and θ a phase factor assumed for simplicity equal for both SP and SF term.

In addition to the tunneling terms, the coupling to the top and bottom gates reads:

$$\begin{aligned} H_g &= \int_{-a}^{a} dx \;\; eV_T \left[-\partial_x \varphi_{R\uparrow}(x) + \partial_x \varphi_{L\downarrow}(x) \right] \\ &+ \;\; eV_B \left[-\partial_x \varphi_{R\downarrow}(x) + \partial_x \varphi_{L\uparrow}(x) \right]. \end{aligned} \tag{15}$$

As anticipated above, V_T and V_B shift the electronic spectrum and their difference breaks the degeneracy between top and bottom boundaries giving $k_F^{(T,B)} = k_F + \kappa_{T,B}$ being $\kappa_{T,B} = KeV_{T,B}/\hbar v_F$. Note that this definition naturally reduces to the non-interacting one[16,18] for $K = 1$, as expected.

The spin current flowing longitudinally in the system is defined as[18]

$$I^{spin}(t) = \frac{\hbar}{2} \left(\dot{N}_{R,\uparrow} - \dot{N}_{L,\downarrow} \right) \tag{16}$$

with number operators

$$N_{\nu,\sigma} = \int_{-\infty}^{+\infty} dx : \Psi^{\dagger}_{\nu,\sigma}(x) \Psi_{\nu,\sigma}(x) : . \tag{17}$$

By evaluating the commutation relations of the tunneling Hamiltonians in Eqs. (12)-(13) with respect to the above number operators one obtains

$$I^{spin}(t) = I^{sp}(t) + I^{sf}(t) \tag{18}$$

with

$$I^{sp}(t) = -\frac{i\hbar}{2} \sum_{\sigma=\uparrow,\downarrow} \int_{-\infty}^{+\infty} dx \gamma_{sp}(x,t) \Psi^{\dagger}_{R,\sigma}(x) \Psi_{L,\sigma}(x) + \text{h.c.} \tag{19}$$

and

$$I^{sf}(t) = -\frac{i\hbar}{2} \sum_{\nu=R,L} \xi_{\nu} \int_{-\infty}^{+\infty} dx \gamma_{sf}(x,t) \Psi^{\dagger}_{\nu,\uparrow}(x) \Psi_{\nu,\downarrow}(x) + \text{h.c.} \tag{20}$$

the SP and SF contributions to the current respectively.

It is worth noting that the current in Eq. (18) was already evaluated in Refs. 11,12 with time independent spin tunneling contribution only.

Here we focus only on the spin current, however the charged current flowing into the system can be obtained in an analogous way by exploiting the relations derived in the so called XYZ decomposition[10,26] that holds for helical edge states in a four-terminal setup.

B. Spin current

The expectation value of the spin current in Eq. (18) is given, according to the Keldysh contour formalism (see Refs. 27–29 and references therein for detailed discussions), by

$$\langle I^{spin}(t)\rangle = \sum_{j=sp,sf} \langle I^j(t)\rangle \tag{21}$$

with

$$\langle I^j(t)\rangle = \frac{1}{2}\sum_{\eta=\pm}\langle \mathcal{T}_K \left\{ I^j(t^\eta) e^{-i\int_c dt_1 \mathcal{H}^j(t_1)}\right\}\rangle \tag{22}$$

where all the operators have to be considered in the interaction picture with respect to $\mathcal{H}_{eff}$ in Eq. (11). The time-ordering along the Keldysh contour $\mathcal{C}$ is indicated by $\mathcal{T}_K$ and $\eta = \pm$ labels the upper and the lower branch of the contour respectively.

At the first order in the total tunneling Hamiltonian[30] one has

$$\langle I^j(t)\rangle = -\frac{i}{2}\sum_{\eta,\eta_1=\pm}\eta_1 \int_{-\infty}^{+\infty} dt_1 \langle T_K I^j(t^\eta)\mathcal{H}^j(t_1^{\eta_1})\rangle \tag{23}$$

where the thermal average is taken with respect to $\mathcal{H}_{eff}$.

Due to the peculiar time dependence of the tunneling amplitudes in Eq. (15), the spin current in Eq. (23) is characterized by both a DC and an AC component (the latter with period 2ω).[31] In the following we will focus only on the DC part. It can be written as the sum of SP and SF contribution, namely

$$\langle I^{spin}_{DC}(\omega)\rangle = \langle I^{sp}_{DC}(\omega)\rangle + \langle I^{sf}_{DC}(\omega)\rangle \tag{24}$$

where

$$\langle I^{sp}_{DC}(\omega)\rangle = \frac{i\hbar\lambda_{sp}^2}{2\pi^2\alpha^2}\sin\phi_{\rm FP}\sin\theta \int_{-\infty}^{+\infty} d\tau \sin(\omega\tau) e^{[\mathcal{W}_R(2a,\tau)+\mathcal{W}_L(2a,\tau)]} \tag{25}$$

and

$$\langle I^{sf}_{DC}(\omega)\rangle = \frac{i\hbar\lambda_{sf}^2}{4\pi^2\alpha^2}\sin\phi_{\rm AB}\sin\theta \sum_{\nu=R,L}\int_{-\infty}^{+\infty} d\tau \sin(\omega\tau) e^{2\mathcal{W}_\nu(2a,\tau)} \tag{26}$$

with $\phi_{\rm FP/AB} = 2\left(k_F^{(1)} \pm k_F^{(2)}\right)a$ Fabry-Pèrot and Aharonov-Bohm like phase factors.[16–18]

It is worth to note that a non zero phase difference in the time dependence of the tunneling amplitudes of the two QPCs ($\theta \neq 0$) is crucial in order to have a DC component of the spin current. This is in agreement with the general statements of the parametric pumping.[32]

The bosonic Green's functions that appear in the Kernel of the integrals above are[33–35]

$$\mathcal{W}_R(x,t) = c_K^{(+)}\mathcal{W}_+(x,t) + c_K^{(-)}\mathcal{W}_-(x,t) \tag{27}$$

$$\mathcal{W}_L(x,t) = c_K^{(-)}\mathcal{W}_+(x,t) + c_K^{(+)}\mathcal{W}_-(x,t), \tag{28}$$

with

$$\mathcal{W}_\pm(x,t) = \mathcal{W}\left(t \mp \frac{x}{v}\right) \tag{29}$$

and

$$\mathcal{W}(t) = \ln\left[\frac{\left|\Gamma\left(1+\frac{k_BT}{\omega_c} - ik_BTt\right)\right|^2}{\Gamma^2\left(1+\frac{k_BT}{\omega_c}\right)(1+i\omega_c t)}\right]. \tag{30}$$

Here

$$c_K^{(\pm)} = \frac{1}{4}\left(\sqrt{K} \pm \frac{1}{\sqrt{K}}\right)^2 \tag{31}$$

are the interaction dependent tunneling coefficients, $\Gamma(x)$ is the Euler Gamma function[36], T the temperature and $\omega_c = v/\alpha$ the energy bandwidth. The latter quantity fixes the limit of validity of the helical Luttinger liquid picture and can be related to the energy gap between the bulk conduction and valence bands of the heterostructure which, in realistic experimental setup[6,13], is $\Delta \approx 30$ meV. According to this assumption one has $\omega_c \sim \Delta/\hbar \approx 50$ GHz.

1. Zero temperature

At zero temperature, Eq. (30) reduces to

$$\mathcal{W}^{(0)}(t) = -\ln(1+i\omega_c t) \tag{32}$$

and the integrals in Eqs. (25)-(26) can be evaluated. The SP term can be written as

$$\langle I^{sp}_{DC}\rangle = \frac{\lambda_{sp}^2\hbar}{4\pi^2\alpha^2}\sin\theta\sin\phi_{\rm FP} H^{(0)}\left(d_K, K\omega/\omega_0\right)\tilde{\mathcal{P}}^{(0)}_{2d_K}(\omega) \tag{33}$$

where

$$d_K = c_K^{(+)} + c_K^{(-)} = \frac{1}{2}\left(K + \frac{1}{K}\right) \tag{34}$$

and $\omega_0 = v_F/2a$.

The modulating function is[37,38]

$$H^{(0)}(\xi,x) = \sqrt{\pi}\frac{\Gamma(2\xi)}{\Gamma(\xi)}\frac{\mathcal{J}_{\xi-\frac{1}{2}}(x)}{(2x)^{\xi-\frac{1}{2}}}, \tag{35}$$

with $\mathcal{J}_{\xi-\frac{1}{2}}(x)$ the Bessel function of the first kind[36], while

$$\tilde{\mathcal{P}}^{(0)}_\xi(E) = \frac{2\pi}{\Gamma(\xi)\omega_c}\left(\frac{E}{\omega_c}\right)^{\xi-1} e^{-E/\omega_c}\theta(E) \tag{36}$$

is the Fourier transform of the zero temperature electronic Green's function $\mathcal{P}^{(0)}_\xi(t) = e^{\xi\mathcal{W}^{(0)}(t)}$.

Note that the function $\tilde{\mathcal{P}}^{(0)}_{2d_K}$ also appears in the calculation of the spin current in the single contact geometry

(both point-like and extended) for a two-terminal configuration with source and drain at different voltage leading to a characteristic power-law behavior.[11,12]

In an analogous way the SF contribution reads

$$\langle I^{sf}_{DC}\rangle = \frac{\lambda^2_{sf}\hbar}{4\pi^2\alpha^2}\sin\theta\sin\phi_{\rm AB} J^{(0)}\left(2c_K^{(+)},2c_K^{(-)},K\omega/\omega_0\right)\tilde{\mathcal{P}}^{(0)}_{2d_K}(\omega), \quad (37)$$

where we introduced the new modulating function

$$J^{(0)}(\xi_1,\xi_2,x) = \frac{1}{2}\left[e^{-ix}{}_1F_1\left(\xi_1,\xi_1+\xi_2;2ix\right) + e^{-ix}{}_1F_1\left(\xi_2,\xi_1+\xi_2;2ix\right)\right] \quad (38)$$

with ${}_1F_1(a,b;z)$ the Kummer Hypergeometric confluent function[36]. Note that the above function admits the limit $J^{(0)}(2,0,x)=\cos x$ and[39] $J^{(0)}(\xi,\xi,x)=H^{(0)}(\xi,x)$.

2. Finite temperature

At finite temperature, as long as $k_BT \ll \hbar\omega_c$ and $\omega_c t \gg 1$, one has

$$\mathcal{W}(t) \approx \frac{\pi k_B T t}{\sinh(\pi k_B T t)}. \quad (39)$$

Also in this case it is possible to write the SP and SF contributions in a factorized way as

$$\langle I^{sp}_{DC}\rangle = \frac{\lambda^2_{sp}\hbar}{4\pi^2\alpha^2}\sin\theta\sin\phi_{\rm FP}H\left(d_K,K\omega/\omega_0,Kk_BT/\hbar\omega_0\right)\left[\tilde{\mathcal{P}}_{2d_K}(\omega,T)-\tilde{\mathcal{P}}_{2d_K}(-\omega,T)\right] \quad (40)$$

and

$$\langle I^{sf}_{DC}\rangle = \frac{\lambda^2_{sf}\hbar}{4\pi^2\alpha^2}\sin\theta\sin\phi_{\rm AB} J\left(2c_K^{(+)},2c_K^{(-)},K\omega/\omega_0,Kk_BT/\hbar\omega_0\right)\left[\tilde{\mathcal{P}}_{2d_K}(\omega,T)-\tilde{\mathcal{P}}_{2d_K}(-\omega,T)\right]. \quad (41)$$

The finite temperature modulating functions are[26,37]

$$H(\xi,\rho,\tau)=2\pi\frac{\Gamma(2\xi)}{\Gamma(\xi)}\frac{e^{-2\pi\xi\tau}}{\sinh\left(\frac{\rho}{2\tau}\right)}\Im\left\{\frac{e^{i\rho}}{\Gamma\left(\xi+i\frac{\rho}{2\pi\tau}\right)\Gamma\left(1-i\frac{\rho}{2\pi\tau}\right)}{}_2F_1\left(\xi,\xi-i\frac{\rho}{2\pi\tau},1-i\frac{\rho}{2\pi\tau};e^{-4\pi\tau}\right)\right\} \quad (42)$$

and

$$J(\xi_1,\xi_2,\rho,\tau) = \pi\frac{\Gamma\left(2(\xi_1+\xi_2)\right)}{\sinh\left(\frac{\rho}{2\tau}\right)}\Im\left\{\frac{e^{-4\pi\xi_1\tau}}{\Gamma(2\xi_2)}\frac{e^{-i\rho}}{\Gamma\left(2+i\frac{\rho}{2\pi\tau}\right)\Gamma\left(\xi_1+\xi_2-i\frac{\rho}{2\pi\tau}\right)}{}_2F_1\left(2\xi_1,\xi_1+\xi_2+i\frac{\rho}{2\pi\tau},2+i\frac{\rho}{2\pi\tau};e^{-4\pi\tau}\right) - \frac{e^{-4\pi\xi_2\tau}}{\Gamma(2\xi_1)}\frac{e^{i\rho}}{\Gamma\left(-i\frac{\rho}{2\pi\tau}\right)\Gamma\left(\xi_1+\xi_2-i\frac{\rho}{2\pi\tau}\right)}{}_2F_1\left(2\xi_2,\xi_1+\xi_2-i\frac{\rho}{2\pi\tau},-i\frac{\rho}{2\pi\tau};e^{-4\pi\tau}\right)\right\}, \quad (43)$$

where $\Im\{...\}$ indicates the imaginary part and ${}_2F_1(a,b,c;z)$ is the hypergeometric function.[36] The finite temperature electron Green's function is (for $\hbar E, k_BT \ll \hbar\omega_c$)

$$\tilde{\mathcal{P}}_\xi(E,T) = \left(\frac{2\pi}{\beta\omega_c}\right)^{\xi-1}\frac{e^{\frac{\hbar E}{2k_BT}}}{\omega_c}\mathcal{B}\left[\frac{\xi}{2}-i\frac{\hbar E}{2\pi k_BT},\frac{\xi}{2}+i\frac{\hbar E}{2\pi k_BT}\right] \quad (44)$$

being $\mathcal{B}[a,b]$ the Euler Beta function.[36] Obviously, according with the above definitions, one has $H(\xi,\rho,0)=H^{(0)}(\xi,\rho)$ and $J(\xi_1,\xi_2,\rho,0)=J^{(0)}(\xi_1,\xi_2,\rho)$.

C. Universality of the pumped spin

The pumped spin is obtained by integrating the DC spin current over a period and one can immediately infer that it is proportional to the area in the parameter space encircled by the pumping parameters, i.e. $\frac{\hbar}{2}\lambda_i^2\sin\theta$, where $i=sf,sp$. Let us note that in the limit of low pumping frequencies $\omega \ll \omega_0$ ($\omega_0 = v_F/2a$), the transport problem is equivalent to consider a scattering off a single impurity localized at $x=0$. By using the Kane and Fisher argument,[40] when considering repulsive interaction $K<1$, the impurity is a relevant perturbation in the infrared limit and thus in the presence of a small bias all the current is backscattered or spin-flipped. For the spin pump this picture implies the maximal pump-

ing response in the adiabatic limit, i.e. the charge or the spin pumped per cycle is quantized. In the case of spinless particles this has been exactly proved in Ref. 20 for $K = 1/2$ where the problem can be mapped to the time dependent scattering involving free chiral fermions and an impurity state.

III. RESULTS

A. Modulating functions

Before entering into the details of the behavior of the spin current, it is useful to analyze the peculiar forms of the modulating functions both at zero and finite temperature. Fig. 2 (a) shows $H^{(0)}$ for different values of the interaction strength K as a function of ω/ω_0. As already discussed in Ref. 37 in the framework of the interferometric properties of the fractional quantum Hall effect, it shows an oscillating and rapidly decaying behavior as a function of the pumping frequency due to the presence of the Bessel function. These oscillations are related to the finite distance between the QPCs. For very close point contacts this behavior disappears. The envelope of the curves decreases algebraically as $(\omega/\omega_0)^{-d_K}$ (see Eq. (34). The positions of the zeroes move to higher frequencies by decreasing K and consequently the number of observed oscillations in the considered range of frequencies decrease by increasing the interaction. An analogous scenario can be found for the modulating function $J^{(0)}$ (see Fig. 2 (b)) that is related to the SF tunneling processes. However, in this case, the oscillations are only slightly suppressed at high frequency.

The comparison between the zero temperature and the finite temperature cases is shown in Fig. 3 for $K = 0.6$ (analogous results can be found for other values of the interaction). It is possible to note that, for $T \ll T_0 = \hbar\omega_0/k_B$, oscillations of H in Eq. (42) (see Fig. 3 (a)) are progressively suppressed by increasing the temperature. However, the periodicity and the zeroes positions are not affected. In the same temperature regime the function J in Eq. (43) is only slightly affected by the temperature with respect to H, as can be seen in Fig. 3 (b), so spin-flipping tunneling terms are quite robust. For $T \gg T_0 = \hbar\omega_0/k_B$ the features of both modulating functions are washed out and additional tunneling processes need to be taken into account.[26]

Note that assuming $a \approx 1$ μm and $v_F \approx 5 \times 10^5$ m/s, as appears from experiments[6,11,13], one obtains $\omega_0 \approx 250$ MHz[41] and consequently $T_0 \approx 2$ K. Being the typical temperature at which experiments are carried out[6,7] $T \approx 30$ mK it is possible to conclude that thermal effects can be reasonably neglected in the relevant experimental cases. This allows us to focus in the following on the zero temperature case.

We also note that at low frequency ($\omega \ll \omega_0$), the effect of the modulating functions is unimportant ($H, J \approx 1$).[19] Moreover for high enough frequency the SP contribution disappears and the physics is dominated by SF tunneling processes. This fact is a consequence of the differences in the interference paths induced by the helical properties of the edge states.[16,18,26]

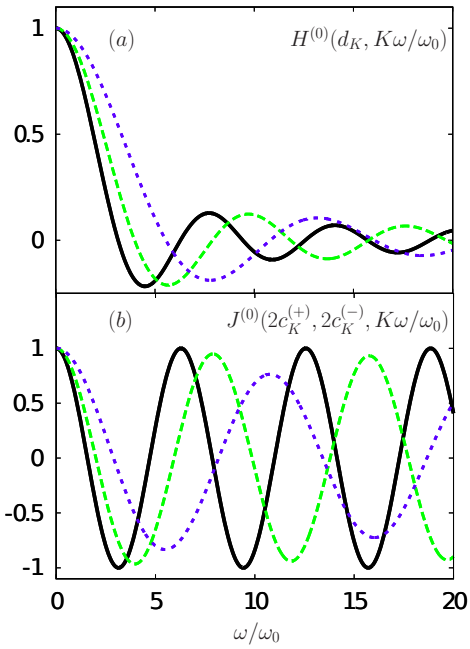

Figure 2: (color online) Modulating functions (a) $H^{(0)}(d_K, K\omega/\omega_0)$ and (b) $J^{(0)}(2c_K^{(+)}, 2c_K^{(-)}, K\omega/\omega_0)$ as a function of ω/ω_0 for $K = 1$ (non-interacting case, full black curve), $K = 0.8$ (dashed green curve) and $K = 0.6$ (short dashed blue curve).

B. Current

The evolution of the zero temperature SP and SF current contributions as a function of the pumping frequency ω is shown in Fig. 4 for different interactions and for a peculiar combination of the Fabry-Pérot and Aharonov-Bohm phases ($\phi_{\rm FP} = \phi_{\rm AB} = \pi/4 \pmod{2\pi}$). It is possible to note the emergence of the power-law behavior typical of the helical Luttinger liquid $\tilde{\mathcal{P}}^{(0)}_{2d_K}(\omega) \propto (\omega/\omega_c)^{K+\frac{1}{K}-1}$, already predicted for the current as a function of the source-drain bias[11,12], but strongly modulated here by the presence of the oscillating functions $H^{(0)}$ (Fig. 4 (a)) and $J^{(0)}$ (Fig. 4 (b)).

Fig. 5 shows the total DC pumped spin current. According to the previous considerations, at high frequency, it is driven only by the SF contribution due to the algebraic damping of the SP one, therefore a detailed study of this regime can provide important information about the role played by this kind of processes in the dynamics of the system.

Even more interesting is the dependence of the current on the Fabry-Pérot and Aharonov-Bohm phase as a function of the pumping frequency and the interaction.

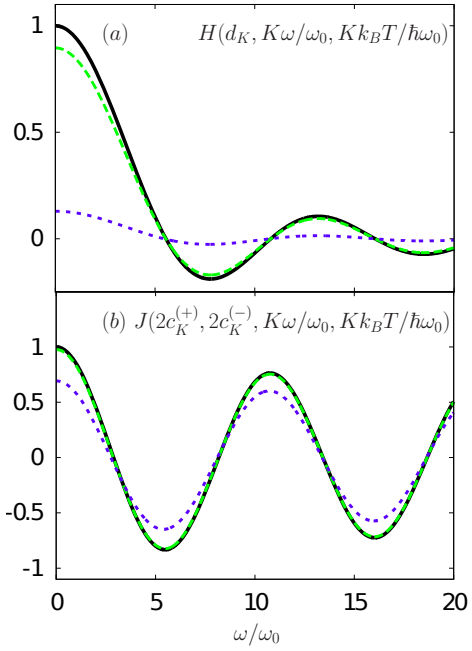

Figure 3: (Color online) Modulating functions as a function of ω/ω_0 for $K = 0.6$ at various temperatures: $k_BT = 0$ (full black curve), $k_BT = 0.2\hbar\omega_0$ (dashed green curve) and $k_BT = \hbar\omega_0$ (short dashed blue curve). (a) $H(d_K, K\omega/\omega_0, Kk_BT/\hbar\omega_0)$ and (b) $J(2c_K^{(+)}, 2c_K^{(-)}, K\omega/\omega_0, Kk_BT/\hbar\omega_0)$.

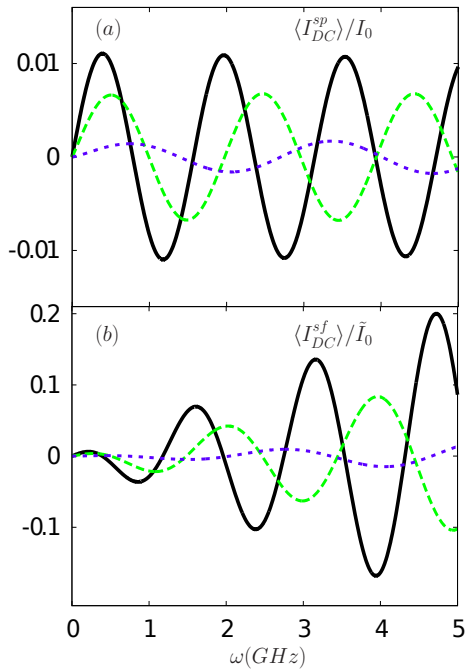

Figure 4: (Color online) (a) SP and (b) SF contributions to the DC spin current (in units of $I_0 = \frac{\lambda_{sp}^2\hbar}{4\pi^2\alpha v_F}\sin\theta$ and $\tilde{I}_0 = \frac{\lambda_{sf}^2\hbar}{4\pi^2\alpha v_F}\sin\theta$ respectively) as a function of ω (in GHz) for: $K = 1$ (non-interacting case, full black curves), $K = 0.8$ (dashed green curves) and $K = 0.6$ (short dashed blue curves). Other parameters are: $v_F = 5\times10^5$ m/s, $a = 1$ μm ($\omega_0 = 250$ MHz), $\alpha = 10^{-8}$ m, $\phi_{\rm FP} = \phi_{\rm AB} = \pi/4$ (mod 2π).

As already shown in the non-interacting case this leads to very intriguing patterns.[18] This is due to the different modulation in amplitude and sign of the SP and SF contributions to the spin current. Some examples of these possible patterns are shown in Fig. 6 for various frequencies at fixed interaction ($K = 0.8$). At low pumping frequency (top left panel) both the SP and SF contributions affect the current leading to clear periodicities both in $\phi_{\rm FP}$ and $\phi_{\rm AB}$.[42] The amplitude of the oscillations crucially depends on the ratio $\lambda_{sf}/\lambda_{sp}$. Typically it is reasonable to assume that these tunneling amplitudes have the same order of magnitude with $\lambda_{sp} > \lambda_{sf}$.[16,18]

In this kind of setup it is also possible to tune the pumping frequency in such a way to have a SF contribution to the spin current equal zero, while the SP is present (top right panel); this leads to a clear periodicity only driven by $\phi_{\rm FP}$. The observation of this vertically striped pattern can give a precise indication of the positions of the zeroes of the SF contribution and consequently of the value of the interaction strength. In the opposite case of null SP contribution and SF different from zero horizontally striped patterns appear driven only by $\phi_{\rm AB}$ (not shown). This configuration is typical also of the high frequency regime (bottom panels) where the SP contribution becomes negligible due to its algebraic damping. The differences in the patterns between the left and right bottom panels depend on the sign of the modulating function J. The strong dependence of the interference path on interaction can be seen in Fig. 7 that compares the interacting (left panel) and non-interacting (right panel) case.

It is worth to note that the patterns of interference described above can be observed only if both SP and SF tunneling processes occurring at the QPCs are present.

IV. CONCLUSIONS

We proposed a two QPCs experimental setup involving helical edge states of a two dimensional topological insulator. Here, a DC pumped spin current is induced by periodically modulating in time SP and SF electron tunneling amplitudes out of phase. We analyzed the different modulating functions associated to these processes both at zero and finite temperature. We discussed also on the universality of the spin pumped in a period. We found that the power-law behavior typical of the helical Luttinger liquid expected for the spin current in a single QPC is strongly affected by interference effects and interaction strenght. We investigated the interference patterns created by Fabry-Pérot and Aharonov-Bohm phases induced by external gates connected to the edges. The measurement of their features, and in particular the locations

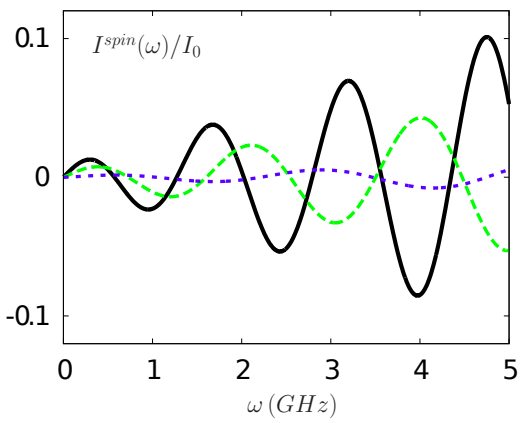

Figure 5: (Color online) Spin current $I_{spin}(\omega)$ (in units of $I_0 = \frac{\lambda_{sp}^2\hbar}{4\pi^2\alpha v_F}\sin\theta$) as a function of ω (in GHz) for: $K = 1$ (non-interacting case, full black curves), $K = 0.8$ (dashed green curves) and $K = 0.6$ (short dashed blue curves). Other parameters are: $v_F = 5\times10^5$ m/s, $a = 1$ μm ($\omega_0 = 250$ MHz), $\alpha = 10^{-8}$ m, $\lambda_{sf}^2/\lambda_{sp}^2 = 0.5$, $\phi_{\rm FP} = \phi_{\rm AB} = \pi/4$ (mod 2π).

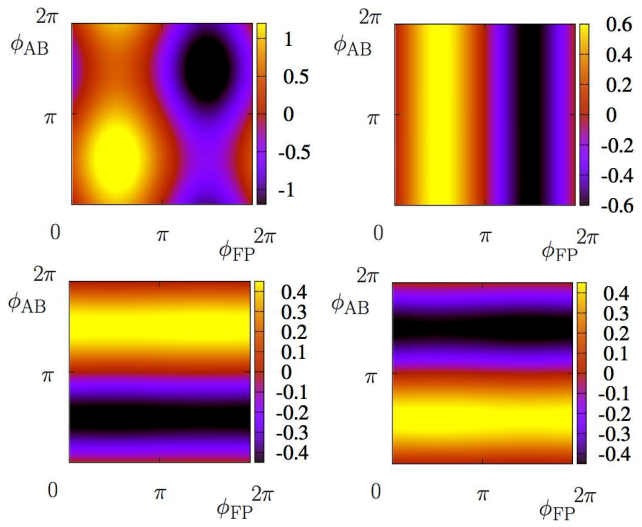

Figure 6: (Color online) Density plot of the spin current $I_{spin}(\omega)$ (normalized with respect to $I_{point}(\omega) = \frac{\lambda_{sp}^2\hbar}{4\pi^2\alpha^2}\sin\theta\tilde{\mathcal{P}}_{2d_K}(\omega)$) as a function of the Fabry-Pérot $\phi_{\rm FP}$ (x axis) and Aharonov-Bohm $\phi_{\rm AB}$ (y axis) phases for different pumping frequency: $\omega = 100$ MHz (top left panel), $\omega = 500$ MHz (top right panel), $\omega = 1$ GHz (botton left panel), $\omega = 2$ GHz (bottom right panel). Other parameters are: $a = 1$ μm, $v_F = 5\times10^5$ m/s, ($\omega_0 = 250$ MHz), $\alpha = 10^{-8}$ m, $\lambda_{sf}^2/\lambda_{sp}^2 = 0.5$, $K = 0.8$.

of their zeros, represents an important tool in order to extract information about the strength of the electron-electron interaction in the system.

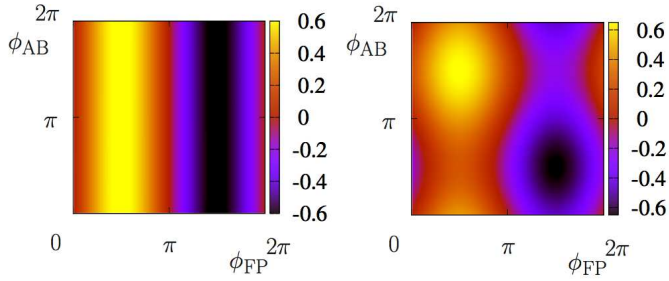

Figure 7: (Color online) Density plot of the spin current $I_{spin}(\omega)$ (normalized with respect to $I_{point}(\omega) = \frac{\lambda_{sp}^2\hbar}{4\pi^2\alpha^2}\sin\theta\tilde{\mathcal{P}}_{2d_K}(\omega)$) as a function of the Fabry-Pérot $\phi_{\rm FP}$ (x axis) and Aharonov-Bohm $\phi_{\rm AB}$ (y axis) phases for interaction $K = 0.8$ (left panel) and $K = 1$ (right panel, non-interacting case). Other parameters are: $a = 1$ μm, $v_F = 5\times10^5$ m/s, ($\omega_0 = 250$ MHz), $\alpha = 10^{-8}$ m, $\lambda_{sf}^2/\lambda_{sp}^2 = 0.5$, $\omega = 500$ MHz.

Acknowledgements

We thank A. Braggio and N. Magnoli for useful discussions. The support of CNR STM 2010 program, EU-FP7 via Grant No. ITN-2008-234970 NANOCTM and CNR-SPIN via Seed Project PGESE001 is acknowledged.

[1] X. -L. Qi and S. -C. Zhang, Rev. Mod. Phys. 83, 1057 (2011).
[2] C. L. Kane and E. J. Mele, Phys. Rev. Lett. **95**, 146802 (2005).
[3] C. L. Kane and E. J. Mele, Phys. Rev. Lett. **95**, 226801 (2005).
[4] B. A. Bernevig and S. -C. Zhang, Phys. Rev. Lett. **96**, 106802 (2006).
[5] B. A. Bernevig, T. L. Hughes, and S. -C. Zhang, Science **314**, 1757 (2006).
[6] M. Konig, S. Weidmann, C. Brune, A. Roth, H. Buhmann, L. W. Molenkampf, X. -L. Qi, and S. -C. Zhang, Science **318**, 766 (2007).
[7] A. Roth, C. Brne, H. Buhmann, L. W. Molenkamp, J. Maciejko, X. -L. Qi, and S. -C. Zhang, Science **325**, 294 (2009).
[8] C. Wu, B. A. Bernevig, and S. -C. Zhang, Phys. Rev. Lett. **96**, 106401 (2006).
[9] M. Z. Hasan and C. L. Kane, Rev. Mod. Phys. **82**, 3045 (2010).
[10] J. C. Y. Teo and C. L. Kane, Phys. Rev. B **79**, 235321 (2009).
[11] A. Strom and H. Johannesson, Phys. Rev. Lett. **102**, 096806 (2009).
[12] G. Dolcetto, S. Barbarino, D. Ferraro, N. Magnoli, and M. Sassetti, Phys. Rev. B **85**, 195138 (2012).
[13] C. -Y. Hou, E. -A. Kim, and C. Chamon, Phys. Rev. Lett. **102**, 076602 (2009).
[14] C.-X. Liu, J. C. Budich, P. Recher, and B. Trauzettel, Phys. Rev. B **83**, 035407 (2011).
[15] T. L. Schmidt, Phys. Rev. Lett. **107**, 096602 (2011).
[16] F. Dolcini, Phys. Rev. B **83**, 165304 (2011).
[17] F. Romeo, R. Citro, D. Ferraro and M. Sassetti, ArXiv: 1208.0514v1.
[18] R. Citro, F. Romeo and N. Andrei, Phys. Rev. B **84**, 161301(R) (2011).
[19] P. Sharma and C. Chamon, Phys. Rev. Lett. **87**, 096401 (2001).
[20] P. Sharma and C. Chamon, Phys. Rev. B **68**, 035321 (2003).
[21] C. Xu and J. E. Moore, Phys. Rev. B **73**, 045322 (2006).
[22] T. Giamarchi, *Quantum Physics in One Dimension*, Oxford University Press, (2003).
[23] E. Miranda, Braz. J. Phys. **33**, 3 (2003).
[24] Note that more complicated multiple electron tunneling processes, namely tunneling of charged and spinful particle pairs[10,15], affect the transport properties of the system for strong enough repulsive or attractive interaction ($K < 1/\sqrt{3}$ or $K > \sqrt{3}$). However in the paper we will focus on a range of parameters where these contributions can be safely neglected.
[25] J. I. Vayrynen and T. Ojanen, Phys. Rev. Lett. **106**, 076803 (2011).
[26] P. Virtanen and P. Recher, Phys. Rev. B **83**, 115332 (2011).
[27] R. Citro, N. Andrei and Q. Niu, Phys. Rev. B **68**, 165312 (2003).
[28] T. Martin, *Les Houches Session LXXXI*, ed. Bouchiat et al, Elsevier, Amsterdam (2005).
[29] A. Kamenev, A. Levchenko, Adv. Phys. **58**, 197 (2009).
[30] Note that this corresponds to the second order in the tunneling amplitudes.
[31] In general, out of the considered perturbative regime, one has $\langle I^{spin}(t)\rangle = \sum_n e^{2in\omega t}\langle I_n^{spin}(\omega)\rangle$ with $\langle I_n^{spin}(\omega)\rangle$ the n-th harmonic of the spin current.
[32] D. J. Thouless, Phys. Rev. B **27**, 6083 (1983).
[33] D. Ferraro, A. Braggio, N. Magnoli and M. Sassetti, Phys. Rev. B **82**, 085323 (2010).
[34] M. Carrega, D. Ferraro, A. Braggio, N. Magnoli and M. Sassetti, Phys. Rev. Lett. **107**, 146404 (2011).
[35] M. Carrega, D. Ferraro, A. Braggio, N. Magnoli and M. Sassetti, New J. Phys. **14**, 023017 (2012).
[36] I. S. Gradshteyn and I. M. Ryzhik *Tables of Integral, Series and Products* Academic, London (1994).
[37] C. Chamon, D. E. Freed, S. A. Kivelson, S. L Sondhi and X. G. Wen, Phys. Rev. B **55**, 2331 (1997).
[38] D. Chevallier, J. Rech, T. Jonckheere, C. Wahl, and T. Martin, Phys. Rev. B **82**, 155318 (2010).
[39] In spite of this identification between the modulating functions in Eqs.(35) and (38) we consider more appropriate to treat them separately in order to better clarify their physical meaning as well as to be consistent with literature.[37]
[40] C. L. Kane and M. P. A. Fisher, Phys. Rev. B **46**, 15233 (1992).
[41] Note that this value of ω_0 guarantees that the relevant features of the pumping can be observed within the regime of validity of the helical Luttinger liquid picture.
[42] Note that the top left panel of Fig. 6 can be seen as the interacting version of Fig. 3 (left panel) of Ref. 18. However the non-interacting analysis shows a richer structure induced by higher order contributions in the tunneling that haven't been taken into account in this paper. This make difficult to directly compare the two pictures.